RSC Advances

PAPER

Cite this: *RSC Adv.*, 2015, **5**, 8022

Aligning 3D nanofibrous networks from self-assembled phenylalanine nanofibers†

Xianfeng Wang,[a] Yi Charlie Chen[b] and Bingyun Li*[a]

Self-assembled synthetic materials are typically disordered, and controlling the alignment of such materials at the nanometer scale may be important for a variety of biological applications. In this study, we have applied directional freeze-drying, for the first time, to develop well aligned three dimensional (3D) nanofibrous materials using amino acid like L-phenylalanine (Phe). 3D free-standing Phe nanofibrous monoliths have been successfully prepared using directional freeze-drying, and have presented a unique hierarchical structure with well-aligned nanofibers at the nanometer scale and an ordered compartmental architecture at the micrometer scale. We have found that the physical properties (*e.g.* nanofiber density and alignment) of the nanofibrous materials could be tuned by controlling the concentration and pH of the Phe solution and the freezing temperature. Moreover, the same strategy (*i.e.* directional freeze-drying) has been successfully applied to assemble peptide nanofibrous materials using a dipeptide (*i.e.* diphenylalanine), and to assemble Phe-based nanofibrous composites using polyethylenimine and poly(vinyl alcohol). The tunability of the nanofibrous structures together with the biocompatibility of Phe may make these 3D nanofibrous materials suitable for a variety of applications, including biosensor templates, tissue scaffolds, filtration membranes, and absorbents. The strategy reported here is likely applicable to create aligned nanofibrous structures using other amino acids, peptides, and polymers.

Received 25th October 2014
Accepted 22nd December 2014

DOI: 10.1039/c4ra13159b

www.rsc.org/advances

Introduction

Most self-assembled synthetic materials are macroscopically disordered, and controlling the alignment of these materials at the nanoscale is important for many applications envisioned for molecular self-assembly.[1–3] Aligning or patterning at the nano- or microscale may extend the order of materials in a predictable manner over large scales, and may dramatically improve material performance and enable materials with new functions.[4–6] The preparation of materials with aligned nano- and microstructures is of interest in a wide range of applications such as tissue engineering, organic electronics, and molecular sensing devices.[7–9] Native tissues are endowed with a highly organized nanofibrous extracellular matrix (ECM) that directs cellular distribution and function.[10] Well-defined three-dimensional (3D) artificial systems of aligned nanofibers are therefore believed to be important in guiding cell growth or tissue regeneration, imitating native ECM.[11,12] Several strategies have been investigated to control the alignment of materials.[13–16] To name a few, liquid-crystalline materials can spontaneously self-organize into long-range aligned structures through supramolecular self-assembly and nano-segregation,[17] and electrospun nanofiber scaffolds with a variety of alignments have been employed to mimic the nanotopography of natural ECM for tissue engineering applications.[11,18–20]

Freeze-drying has recently attracted considerable interest as a general approach to guide nano- or microscale ordering.[7,21,22] Starting with an aqueous solution or dispersion, freezing causes the solutes or solids to be excluded by an advancing ice front into the interstitial spaces between ice crystals. Subsequent drying under vacuum leads to the sublimation of solvent and formation of porous and particulate structures.[23] As a result, the freeze-drying process has certain advantages: (i) water, an environmentally friendly solvent, and ice crystals, serving as a porogen, are green and sustainable. These characteristics are particularly beneficial for biological applications. (ii) During removal of the solvent, no impurities are introduced while the purity of the final product could be improved.[21] (iii) More importantly, by tuning the freeze-drying conditions, complex hierarchical morphologies such as well-aligned channels, honeycombs, and brick-mortar-bridges,[7,24–26] may be achieved. Currently, freeze-drying has been investigated for the fabrication of aligned porous structures using different building blocks, including polymers,[7] nanoparticles,[27] silver nanowires,[28]

[a]*Department of Orthopaedics, School of Medicine, West Virginia University, Morgantown, WV 26506, USA. E-mail: bili@hsc.wvu.edu*

[b]*Department of Biology, Natural Science Division, Alderson-Broaddus University, Philippi, WV 26416, USA*

† Electronic supplementary information (ESI) available: FE-SEM images, AFM image, and diameter distribution of Phe nanofibers obtained by conventional drop-casting method. CO_2 capture performance of Phe nanofibrous monoliths. See DOI: 10.1039/c4ra13159b

hydrogels,[29] or mixtures of such materials.[21,30] Amino acid and peptide building blocks are very attractive biological building blocks, for bionanotechnology applications, owing to their biocompatibility, chemical flexibility and versatility, biological recognition abilities, and straightforward synthesis.[1,31–36] To our knowledge, very few studies have reported the possibility of aligning or patterning materials using freeze-drying of self-assembled amino acids or peptides.

Herein, we report the application of freeze-drying, for the first time, to direct self-assembled L-phenylalanine (Phe) and diphenylalanine (Phe–Phe) nanofibers into 3D well-aligned nanofibrous architectures, and to develop Phe-based nanofibrous composites. The general principle of using freeze-drying strategy to achieve finer control of porous network structures, applied here to Phe and Phe–Phe, is likely applicable to other peptides and materials classes to produce structures of relevance to many practical applications.

Experimental

Materials

Phe, Phe–Phe, Rhodamine B (RhoB), poly(vinyl alcohol) (PVA, M_w = 90 000), and branched polyethylenimine (PEI, average M_w = ~25 000) were purchased from Sigma (St. Louis, MO). Distilled water was used as a solvent. RhoB labeled PEI (RhoB-PEI) was obtained by mixing PEI and RhoB in 50 mM phosphate buffered solution at a molar ratio of 1 : 100 of PEI to RhoB, stirring for 2 h at room temperature, and dialyzing in deionized water using a cellulose dialysis sack with a cutoff of 10 kDa for 2 days. Fresh stock solutions of Phe were prepared by dissolving Phe in distilled water at concentrations of 10, 25, 50, 100, and 150 mM. A Phe–Phe solution was prepared by dissolving Phe–Phe in distilled water with vigorous stirring at a concentration of 2 mM. Phe–PVA and Phe–PEI solutions were obtained by adding PVA or RhoB-PEI, respectively, into 100 mM Phe solution at a Phe/PVA or Phe/RhoB-PEI weight ratio of 5/1.

Conventional drop-casting of Phe, Phe–Phe, Phe–PEI, and Phe–PVA materials

Three μL of Phe, Phe–Phe, Phe–PEI, or Phe–PVA solution was dropped on a clean stainless steel substrate and allowed to dry at 25 °C in a vacuum for 12 h prior to subsequent characterization.

Directional freeze-drying of Phe, Phe–Phe, Phe–PEI, and Phe–PVA materials

1.5 mL of Phe, Phe–Phe, Phe–PEI, or Phe–PVA solution was pipetted into a 2 mL centrifuge tube. The tube was placed into liquid nitrogen or a −20 or −80 °C freezer. Frozen samples were then freeze-dried using a Virtis automatic freeze-dryer.

Characterization

Field emission scanning electron microscopy or FE-SEM (JEOL, JSM-7600F) was performed at 10 kV to characterize the morphology of nanofibrous materials. Before imaging, samples were coated (Hummer IV Sputtering System) with a thin layer of gold to promote conductivity. The diameters of nanofibers were measured using an image analyzer (Adobe Photoshop CS2 9.0). A nanoscope multimode scanning probe microscope (Bruker Instruments) was used for the atomic force microscopy (AFM) measurements. RhoB stained samples were examined under a confocal laser scanning microscopy or CLSM (LSM 510, Carl Zeiss, Jena, Germany). Circular dichroism (CD) spectra were recorded using a Jasco J-810 spectropolarimeter (Japan) with instrument settings of 100 mdeg sensitivity, 1 nm bandwidth, 1 s response time, 1 nm data pitch, and 100 nm min^{-1} scan rate. A total of 50–80 scans were accumulated and averaged in each experiment. Materials were prepared at a concentration of 100 μM and analyzed in a 10 mm quartz cell at 25 °C. The CO_2 capture performance of Phe nanofibrous monoliths was determined using thermal gravimetric analysis (TGA) as we previously reported.[37–39] In brief, samples were placed into the middle of the TGA microbalance quartz-tube reactor and heated to 105 °C in a N_2 atmosphere at a flow of 200 mL min^{-1} for about 60 min. The temperature was then adjusted to 40 °C and pure dry CO_2 was introduced at a gas flow rate of 200 mL min^{-1} until no obvious weight gain was observed. The weight change in mg of the sorbents was recorded and the weight change in percentage was defined as the ratio of the amount of the gas adsorbed over the total amount of CO_2 adsorbed. Adsorption capacity in mmol per (g sorbent) was calculated from the weight change of the samples during adsorption.

Results and discussion

A typical liquid nitrogen freezing process followed by freeze-drying (so called directional freeze-drying) was explored to develop aligned 3D architectures of amino acids (Fig. 1a–e). Phe nanofibers (Fig. S1†) with diameter of ~160 nm and length of tens of micrometers were self-assembled[40,41] and formed a highly aligned nanofibrous architecture. When freezing the Phe

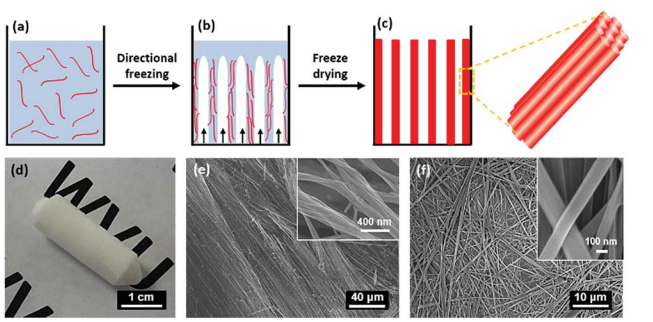

Fig. 1 Formation mechanism and morphology of aligned 3D Phe nanofibrous materials. (a–c) Schematic showing the formation of aligned nanofibers using directional freeze-drying. The Phe nanofibers in the solution are excluded from the freezing front, concentrate and aligned between the orientated solvent crystals. Aligned nanofibrous materials are obtained upon subsequent removal of solvent during the freeze-drying process. (d) Photo image of a freeze-dried 3D Phe nanofibrous monolith. (e) Typical FE-SEM image of Phe nanofibers obtained using directional freeze-drying. Inset is a high magnification image. (d and e) Phe concentration was 100 mM, pH was 5.5, and samples were frozen in liquid nitrogen. (f) Typical FE-SEM image of Phe nanofibers prepared using the conventional drop-casting.

solution in liquid nitrogen, anisotropic ice crystals grew preferentially along the temperature gradient to form parallel "ice fingers", and simultaneously concentrated and aligned the Phe nanofibers from the solidifying solution (Fig. 1b). As a result, Phe nanofiber bundles were formed among the ice fingers (Fig. 1c) and developed into an interconnected 3D compartmental micro-network. Upon removal of the solvent during freeze-drying, a macroscopic free-standing monolith (Fig. 1d) of an interconnected fibrous network with a well-aligned compartmental architecture was obtained (Fig. 1e). Directional freeze-drying seems to be a promising technology for the development of ordered architectures with various types of materials such as polymers, ceramics, nanoparticles, Ag nanowires, and their composites.[7,21] By contrast, nanofibrous materials with randomly distributed Phe nanofibers were formed when conventional drop-casting was applied (Fig. 1f).

The effect of initial Phe solution concentration on microstructures of the 3D nanofibrous monoliths was investigated. All of the monoliths obtained using liquid nitrogen freezing consisted of a 3D aligned nanofibrous network structure, and their nanofibrous network became denser with increasing Phe concentration (Fig. 2). Close examination of the nanofibers revealed that the aligned nanofibers tended to aggregate into bundles with diameters on the order of hundreds of nanometers (Fig. 2d inset). At a Phe concentration of 10 mM, the nanofibers seemed to be much shorter compared to those at concentrations of 25–150 mM and the formed network was noncontinuous and less aligned. Therefore, it seems that the density and alignment of Phe nanofibers can be readily tuned through controlling the initial Phe concentration. One interesting application of aligned nanofibrous materials is to serve as scaffolds for directional growth of biological cells and tissues, and Xie and co-workers found that nanofiber density played an important role in dorsal root ganglia neurite growth (*i.e.* parallel or perpendicular to the direction of fiber alignment) on aligned electrospun nanofibers.[42] The effect of the alignment of Phe nanofibers on biological cell growth may be studied in the future.

The solution pH was also found to play an important role in the formation of Phe nanofibrous materials. Well aligned Phe nanofibrous materials were formed at pH 5.5 and pH 9 (Fig. 3a and b). Clear fibrous structure was observed when the pH was increased to 10 while no nanofibers were observed at pH 11 (Fig. 3c and d). Comparing to pH 5.5, the nanofibers formed at pH 9 aggregated into bundles (Fig. 3a and b). Phe [$C_6H_5CH_2$-$CH(NH_2)COOH$] is an amino acid and the pK_a values of its amino and carboxyl groups are pH 9.09 and pH 2.18, respectively. As a result, Phe exists as a zwitterion [$C_6H_5CH_2CH(NH_3^+)$-COO^-] at pH 5.5 and pH 9 and as $C_6H_5CH_2CH(NH_2)COO^-$ at pH 11. Therefore, our finding suggested that intermolecular electrostatic interactions at pH 5.5 and pH 9 may have played a significant role in the formation of self-assembled Phe nanofibrous materials. Similarly, Singh *et al.* reported that Phe could self-assemble into nanofibers in a zwitterionic state.[43]

Amino acids have been established as promising CO_2 capture materials both as solvent and sorbent.[37,44,45] One issue that limits the application of amino acids as gas sorbent or solvent is the protonation of their amino groups. Addition of a base into the zwitterionic amino acid solution can deprotonate the protonated amino groups and lead to absorption of CO_2. Therefore, the Phe nanofibrous materials obtained at pH 10 and 11 with deprotonated amino group (pK_a of Phe is 9.09) have great potential as sorbents for CO_2 adsorption. The CO_2 capture performance of Phe nanofibrous monoliths demonstrated that the CO_2 capacity of deprotonated Phe nanofibers (pH = 10) was much higher than that of Phe powders (Fig. S2†).

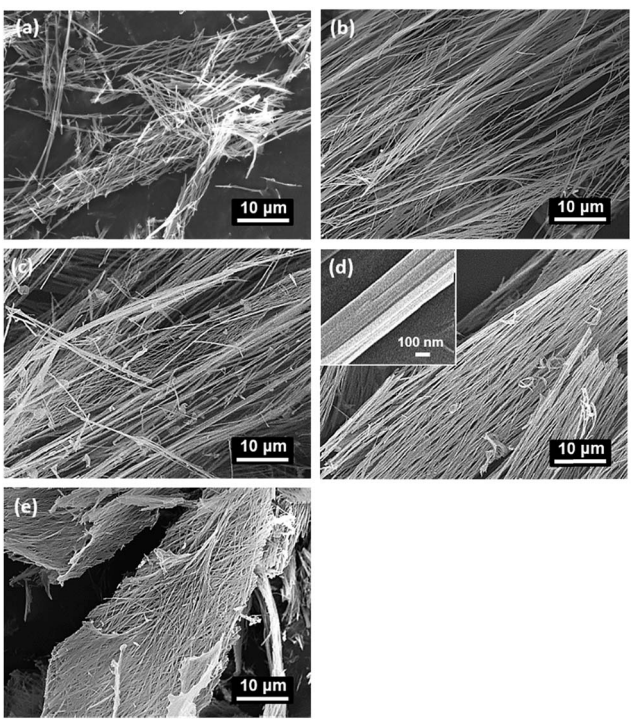

Fig. 2 Microstructures of 3D Phe nanofibrous materials obtained from Phe solutions of (a) 10, (b) 25, (c) 50, (d) 100, and (e) 150 mM, respectively, and frozen with liquid nitrogen. Inset shows higher magnification image.

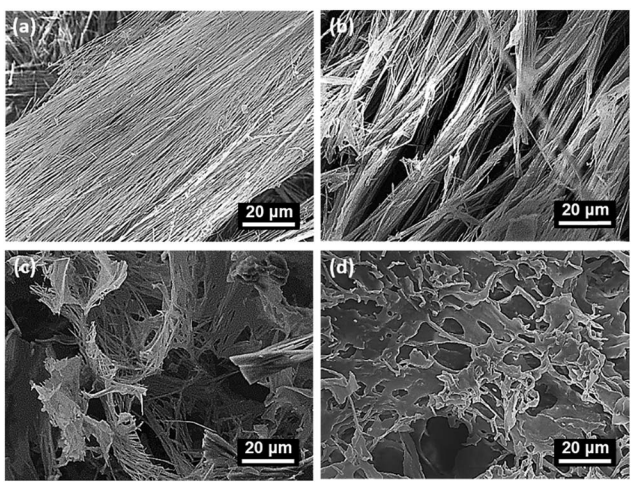

Fig. 3 Phe materials prepared by directional freeze-drying using liquid nitrogen from solution pH of (a) 5.5, (b) 9, (c) 10, and (d) 11. pH was adjusted by NaOH or HCl. Concentration of Phe was 100 mM.

Further, significant differences were observed in the structures of freeze-dried Phe 3D nanofibrous materials prepared at different freezing temperatures (Fig. 4). When frozen at −20 °C, the freeze-dried Phe nanofibrous monolith had a 3D porous architecture with randomly oriented nanofibers (Fig. 4a and b). The nanofibrous network became denser and better aligned with decreasing freezing temperature (Fig. 4c–f), and well aligned, densely packed nanofibrous structures were obtained when the samples were frozen in liquid nitrogen (*i.e.* −196 °C, Fig. 4e and f). These results indicated that reducing freezing temperature may lead to the increase in nanofiber density as well as nanofiber alignment. This finding was supported by the observations by Gao *et al.* who achieved denser and better aligned Ag nanowires at lower freezing temperatures.[28] Wu and Meredith also found that freezing temperature was an important parameter in defining the size of the initial ice crystals which in turn determined the ultimate microstructures of 3D chitin nanofibers.[23] It was proposed that more initial ice crystals would form and the ice crystals would grow faster at lower freezing temperatures.[29,46] At −196 °C, the Phe solution was subject to a significant temperature gradient in the thickness direction, leading to oriented nanofibrous structures (Fig. 4f). At −20 °C, the temperature gradient was much smaller and randomly oriented nanofibrous structures were formed (Fig. 4a and b). These findings emphasize that variations in freezing temperature can result in dramatic changes in microstructures (*e.g.* nanofiber density and alignment) of the final Phe nanofibrous materials.

In this study, the same strategy (*i.e.* directional freeze-drying) was also successfully applied to assemble other nanofibers into 3D well-aligned nanofibrous materials. Nanofibrous materials with well aligned and densely packed nanofibers were developed using a dipeptide, *i.e.* diphenylalanine or Phe–Phe (Fig. 5a). By contrast, randomly distributed nanofibers were formed using the conventional drop-casting approach (Fig. 5b).

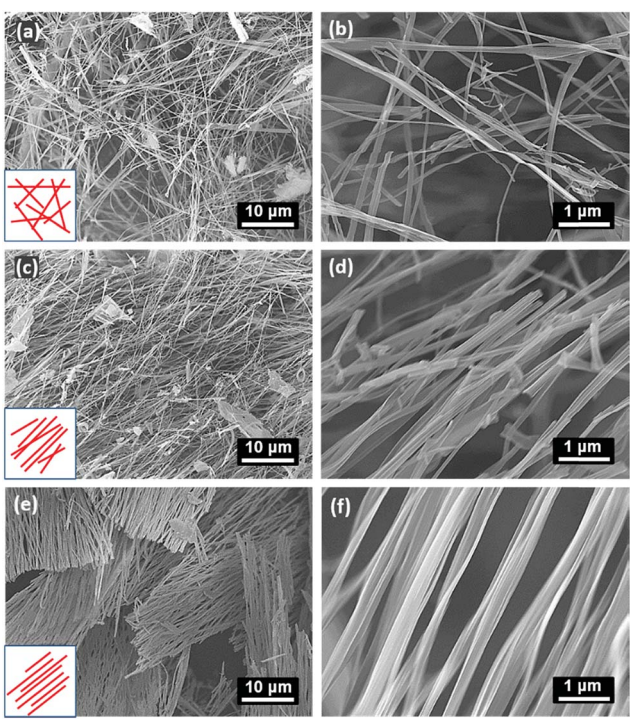

Fig. 4 Microstructures of 3D Phe nanofibrous materials prepared at (a and b) −20, (c and d) −80, and (e and f) −196 °C (liquid nitrogen). Concentration of Phe was 100 mM and pH was 5.5.

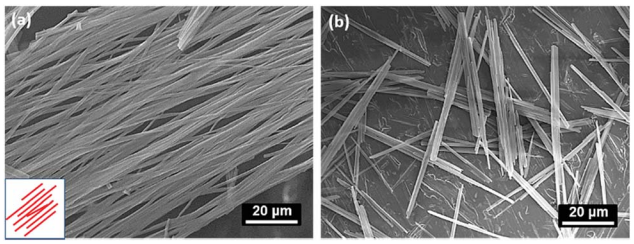

Fig. 5 FE-SEM images of dipeptide Phe–Phe nanofibers formed by (a) directional freeze-drying using liquid nitrogen freezing and (b) conventional drop-casting. Concentration of Phe–Phe was 2 mM and pH was 7.0.

In addition, the same strategy (*i.e.* directional freeze-drying) was successfully applied to develop Phe-based nanofibrous composites. We successfully developed Phe-based nanofibrous composites by introducing polymers like PEI and PVA into Phe nanofibrous networks (Fig. 6). PEI was selected because PEI is an interesting polymer for the constructions of nano-structured architectures for sensing, drug delivery, carbon capture, *etc.*[38,39,47–49] We found that the aligned nanofibrous structure of Phe was maintained in the Phe–PEI composite (Fig. 6a and b) and parallel-wall structures were formed in the Phe–PVA composite (Fig. 6d and e) when directional freeze-drying was applied. By labeling PEI with RhoB, we confirmed that PEI was uniformly distributed within the Phe–PEI nanofibers using CLSM (Fig. 6g). Directional freeze-drying of PVA in liquid nitrogen was reported to develop porous fish-bone structures,[7] different from the fine parallel-wall structures created herein in the Phe–PVA composite. Interestingly, the corresponding high-magnification image (Fig. 6e) confirmed that the Phe–PVA parallel-wall was covered with a dense layer of nanofibers. It seems that PVA parallel-walls served as supports for the self-assembled Phe nanofibers. The secondary structure of Phe–PEI and Phe–PVA composites were found to be similar to that of Phe nanofibers since the CD spectra of Phe–PEI and Phe–PVA presented similar absorption properties as Phe (*i.e.* with a clearly visible absorption at 218 nm, Fig. 6h). This finding may further suggest that the introduction of PEI and PVA did not change the molecule interaction characteristics of the Phe nanofibers; Perween and co-workers recently reported a similar absorption of Phe at 218 nm.[40] Similar to Phe and Phe–Phe, no preferential alignments were observed when conventional drop-casting was used (Fig. 6c and f).

Therefore, our study showed that directional freeze-drying is a simple technique that can be used to produce Phe and Phe-based complex, multicomponent aligned structures without the use of any chemical reagents. More significantly, this approach is advantageous in forming nanofibrous materials for biological applications since it can simultaneously incorporate amino acids or peptides and polymers into aligned nanofibrous composite

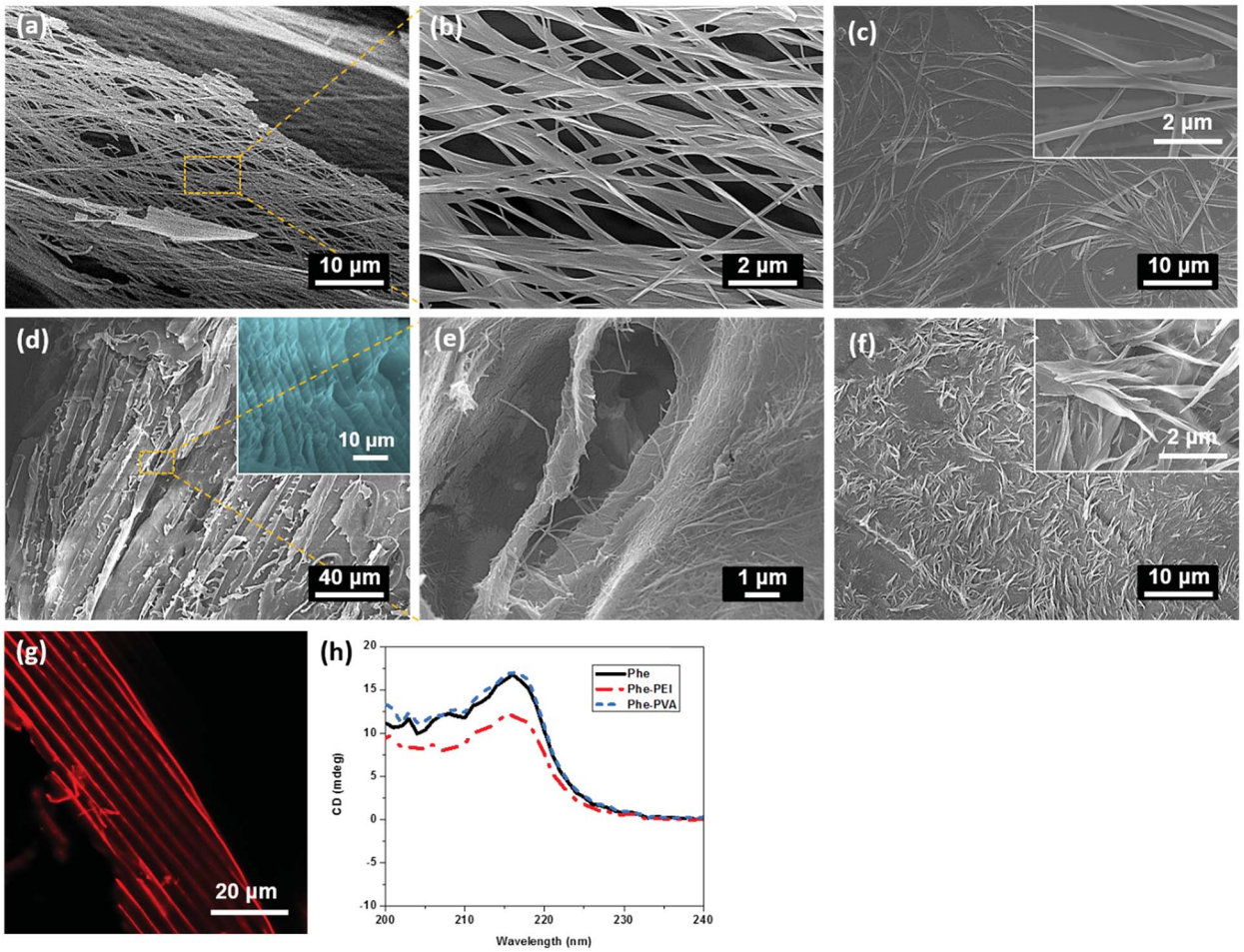

Fig. 6 FE-SEM images of Phe–PEI nanofibrous materials formed by (a and b) directional freeze-drying using liquid nitrogen freezing and (c) conventional drop-casting. Concentration of Phe–PEI solution was 100 mM and Phe/PEI weight ratio was 5/1. (d–f) FE-SEM images of Phe–PVA aligned porous materials formed by (d and e) directional freeze-drying using liquid nitrogen freezing and (f) conventional drop-casting. Concentration of Phe–PVA solution was 100 mM and Phe/PVA weight ratio was 5/1. Inset of (d) shows the cross-section perpendicular to the direction of alignment. Insets of (c) and (f) show higher magnification images. (g) Confocal microscopy image of freeze-dried Phe–PEI nanofibers. PEI was RhoB labeled. (h) CD spectra of Phe, Phe–PEI, and Phe–PVA solutions at a concentration of 100 μM.

structures without the introduction of any toxic by-products. Further studies will focus on the post-treatment (*e.g.* cross-linking) of the 3D nanofibrous materials and the exploration of potential biological applications of such nanofibrous materials.

Conclusions

We successfully developed aligned nanofibrous materials using the amino acid Phe and its dipeptide. Directional freeze-drying was shown to be a simple approach for fabrication of aligned nanofibrous materials, and may offer great flexibility in controlling microstructures of 3D nanofibrous materials. The concentration and pH of the initial Phe concentration and the freezing temperature were found to play an important role in the formation of the aligned nanofibrous materials. The Phe nanofibers were found to be short at the Phe concentration of 10 mM, and long and well aligned at 25–150 mM. Well aligned Phe nanofibrous materials were formed at pH 5.5 and pH 9 while no nanofibers were observed at pH 11; compared to pH 5.5, the nanofibers formed at pH 9 aggregated into bundles. The Phe nanofiber density and alignment were further found to increase with decreasing freezing temperature. When frozen at −20 °C, the nanofibers were almost randomly distributed, while well aligned and densely packed nanofibrous structures were obtained when frozen at −196 °C. To further take advantage of the unique nanofibrous architectures, we also introduced polymers like PEI and PVA into the nanofibrous networks and achieved Phe-based aligned nanofibrous composites. The tunability of the network structure together with the biocompatibility of amino acids makes 3D nanofibrous architecture and its composites suitable candidates in a wide variety of applications, such as reinforcing phases for polymer composites, tissue scaffolds, sensors, and sorbents.

Acknowledgements

The authors wish to acknowledge the support of the West Virginia Higher Education Policy Commission Division of Science

Research PUI Incubator program. We acknowledge use of the WVU Shared Research Facilities. Imaging experiments and image analysis were performed in the West Virginia University Imaging Facility, which is supported in part by the Mary Babb Randolph Cancer Center and NIH grant P30 RR032138 (CoBRE III-After July 1, 2011). The authors thank Suzanne Danley for proofreading.

Notes and references

1 M. Reches and E. Gazit, *Nat. Nanotechnol.*, 2006, **1**, 195–200.
2 Z. H. Zhong, D. L. Wang, Y. Cui, M. W. Bockrath and C. M. Lieber, *Science*, 2003, **302**, 1377–1379.
3 E. Busseron, Y. Ruff, E. Moulin and N. Giuseppone, *Nanoscale*, 2013, **5**, 7098–7140.
4 A. M. Hung and S. I. Stupp, *Nano Lett.*, 2007, **7**, 1165–1171.
5 J. Aizenberg, A. J. Black and G. M. Whitesides, *Nature*, 1999, **398**, 495–498.
6 R. M. Nie, Y. Y. Wang and X. Y. Deng, *ACS Appl. Mater. Interfaces*, 2014, **6**, 7032–7037.
7 H. F. Zhang, I. Hussain, M. Brust, M. F. Butler, S. P. Rannard and A. I. Cooper, *Nat. Mater.*, 2005, **4**, 787–793.
8 D. Chen, Y. E. Miao and T. X. Liu, *ACS Appl. Mater. Interfaces*, 2013, **5**, 1206–1212.
9 Y. L. Xi, H. Dong, K. Sun, H. L. Liu, R. M. Liu, Y. S. Qin, Z. J. Hu, Y. Zhao, F. Q. Nie and S. T. Wang, *ACS Appl. Mater. Interfaces*, 2013, **5**, 4821–4826.
10 D. Silva, A. Natalello, B. Sanii, R. Vasita, G. Saracino, R. N. Zuckermann, S. M. Doglia and F. Gelain, *Nanoscale*, 2013, **5**, 704–718.
11 X. F. Wang, B. Ding and B. Y. Li, *Mater. Today*, 2013, **16**, 229–241.
12 T. Fujie, S. Ahadian, H. Liu, H. X. Chang, S. Ostrovidov, H. K. Wu, H. Bae, K. Nakajima, H. Kaji and A. Khademhosseini, *Nano Lett.*, 2013, **13**, 3185–3192.
13 A. Demortiere, A. Snezhko, M. V. Sapozhnikov, N. Becker, T. Proslier and I. S. Aranson, *Nat. Commun.*, 2014, **5**, 3117.
14 M. Muthukumar, C. K. Ober and E. L. Thomas, *Science*, 1997, **277**, 1225–1232.
15 J. W. Xie, M. R. MacEwan, W. Z. Ray, W. Y. Liu, D. Y. Siewe and Y. N. Xia, *ACS Nano*, 2010, **4**, 5027–5036.
16 S. M. Zhang, M. A. Greenfield, A. Mata, L. C. Palmer, R. Bitton, J. R. Mantei, C. Aparicio, M. O. de la Cruz and S. I. Stupp, *Nat. Mater.*, 2010, **9**, 594–601.
17 T. Kato, N. Mizoshita and K. Kishimoto, *Angew. Chem., Int. Ed.*, 2006, **45**, 38–68.
18 D. Li and Y. N. Xia, *Adv. Mater.*, 2004, **16**, 1151–1170.
19 A. Greiner and J. H. Wendorff, *Angew. Chem., Int. Ed.*, 2007, **46**, 5670–5703.
20 A. Hasan, A. Memic, N. Annabi, M. Hossain, A. Paul, M. R. Dokmeci, F. Dehghani and A. Khademhosseini, *Acta Biomater.*, 2014, **10**, 11–25.
21 L. Qian and H. F. Zhang, *J. Chem. Technol. Biotechnol.*, 2011, **86**, 172–184.
22 Y. Chen, Y. X. Zhang, J. Baker, P. Majumdar, Z. B. Yang, M. F. Han and F. L. Chen, *ACS Appl. Mater. Interfaces*, 2014, **6**, 5130–5136.
23 J. Wu and J. C. Meredith, *ACS Macro Lett.*, 2014, **3**, 185–190.
24 Z. Xu, Y. Zhang, P. Li and C. Gao, *ACS Nano*, 2012, **6**, 7103–7113.
25 M. C. Gutiérrez, M. L. Ferrer and F. del Monte, *Chem. Mater.*, 2008, **20**, 634–648.
26 E. Munch, M. E. Launey, D. H. Alsem, E. Saiz, A. P. Tomsia and R. O. Ritchie, *Science*, 2008, **322**, 1516–1520.
27 H. Zhang, J. Y. Lee, A. Ahmed, I. Hussain and A. I. Cooper, *Angew. Chem., Int. Ed.*, 2008, **47**, 4573–4576.
28 H. L. Gao, L. Xu, F. Long, Z. Pan, Y. X. Du, Y. Lu, J. Ge and S. H. Yu, *Angew. Chem., Int. Ed.*, 2014, **53**, 4561–4566.
29 H. Bai, A. Polini, B. Delattre and A. P. Tomsia, *Chem. Mater.*, 2013, **25**, 4551–4556.
30 H. B. Chen, B. S. Chiou, Y. Z. Wang and D. A. Schiraldi, *ACS Appl. Mater. Interfaces*, 2013, **5**, 1715–1721.
31 L. Adler-Abramovich, D. Aronov, P. Beker, M. Yevnin, S. Stempler, L. Buzhansky, G. Rosenman and E. Gazit, *Nat. Nanotechnol.*, 2009, **4**, 849–854.
32 J. X. Wang, Q. Lei, G. F. Luo, T. T. Cai, J. L. Li, S. X. Cheng, R. X. Zhuo and X. Z. Zhang, *Langmuir*, 2013, **29**, 6996–7004.
33 J. Ryu, S. W. Kim, K. Kang and C. B. Park, *ACS Nano*, 2010, **4**, 159–164.
34 J. N. Luo and Y. W. Tong, *ACS Nano*, 2011, **5**, 7739–7747.
35 A. Acharya, B. Ramanujam, A. Mitra and C. P. Rao, *ACS Nano*, 2010, **4**, 4061–4073.
36 W. Li, Y. Kim and M. Lee, *Nanoscale*, 2013, **5**, 7711–7723.
37 X. Wang, N. G. Akhmedov, Y. Duan, D. Luebke, D. Hopkinson and B. Li, *ACS Appl. Mater. Interfaces*, 2013, **5**, 8670–8677.
38 B. Y. Li, B. B. Jiang, D. J. Fauth, M. L. Gray, H. W. Pennline and G. A. Richards, *Chem. Commun.*, 2011, **47**, 1719–1721.
39 B. Jiang, V. Kish, D. J. Fauth, M. L. Gray, H. W. Pennline and B. Li, *Int. J. Greenhouse Gas Control*, 2011, **5**, 1170–1175.
40 S. Perween, B. Chandanshive, H. C. Kotamarthi and D. Khushalani, *Soft Matter*, 2013, **9**, 10141–10145.
41 L. Adler-Abramovich, L. Vaks, O. Carny, D. Trudler, A. Magno, A. Caflisch, D. Frenkel and E. Gazit, *Nat. Chem. Biol.*, 2012, **8**, 701–706.
42 J. W. Xie, W. Y. Liu, M. R. MacEwan, P. C. Bridgman and Y. N. Xia, *ACS Nano*, 2014, **8**, 1878–1885.
43 V. Singh, R. K. Rai, A. Arora, N. Sinha and A. K. Thakur, *Sci. Rep.*, 2014, **4**, 3875.
44 A. Liu, R. Ma, C. Song, Z. Yang, A. Yu, Y. Cai, L. He, Y. Zhao, B. Yu and Q. Song, *Angew. Chem., Int. Ed.*, 2012, **51**, 11306–11310.
45 D. M. Munoz, A. F. Portugal, A. E. Lozano, J. G. de la Campa and J. de Abajo, *Energy Environ. Sci.*, 2009, **2**, 883–891.
46 S. Deville, E. Saiz, R. K. Nalla and A. P. Tomsia, *Science*, 2006, **311**, 515–518.
47 X. F. Wang, B. Ding, G. Sun, M. R. Wang and J. Y. Yu, *Prog. Mater. Sci.*, 2013, **58**, 1173–1243.
48 X. F. Wang, B. Ding, J. Y. Yu and M. R. Wang, *J. Mater. Chem.*, 2011, **21**, 16231–16238.
49 B. Ding, X. F. Wang, J. Y. Yu and M. R. Wang, *J. Mater. Chem.*, 2011, **21**, 12784–12792.